Higher-order assumed stress quadrilateral element for the Mindlin plate bending problem

Tan Li[*1], Zhaohui Qi[1], Xu Ma[1] and Wanji Chen[2]

[1]*State Key Laboratory for Structural Analysis of Industrial Equipment, Department of Engineering Mechanics, Dalian University of Technology, Dalian, 116023, China*
[2]*Key Laboratory of Liaoning Province for Composite Structural Analysis of Aero craft and Simulation, Shenyang Aerospace University, Shenyang 110136, China*

Abstract.   In this paper an 8-node quadrilateral assumed stress hybrid Mindlin plate element with 39β is presented. The formulation is based on complementary energy principle. The proposed element is free of shear locking and is capable of passing all the patch tests, especially the non-zero constant shear enhanced patch test. To accomplish this purpose, special attention is devoted to selecting boundary displacement interpolation and stress approximation in domain. The arbitrary order Timoshenko beam function is successfully used to derive the boundary displacement interpolation. According to the equilibrium equations, an appropriate stress approximation is rationally derived. Particularly, in order to improve element's accuracy, the assumed stress field is derived by employing 39β rather than conventional 21β. The resulting element can be adopted to analyze both moderately thick and thin plates, and the convergence for the very thin case can be ensured theoretically. Excellent element performance is demonstrated by a wide of experimental evaluations.

Keywords: hybrid stress element; Mindlin plate; arbitrary order Timoshenko beam function; enhanced patch test

1. Introduction

The finite element method has become the most popular and widely used computational method in science and engineering. However, the convergence theory of the finite element is still not complete. Patch test has long been recognized as a convergence criterion (Wang 2001) that assures the convergence of the finite element. In fact, the applications of the existing patch test are limited in 2D/3D elasticity and thin plate problem with homogeneous differential equations. It is difficult to accurately assess the convergence of the problem with non-homogeneous differential equations, for example, none of the current existing Mindlin plate elements can pass the constant shear patch test, such as $w=1+x+y$, $\theta_x=-1$, $\theta_y=-1$. The convergence of element is an unavoidable issue which has been a longstanding problem. Investigators who know this problem on Mindlin plate have devoted themselves to this issue, but could not find a feasible solution, while quite a

---

∗Corresponding author, Ph.D. Student, E-mail: litan910@163.com

few researchers may not be consciously aware of the difficulty of the problem. Mindlin plate elements are widely used by commercial software, many authors think there is no problem, but it is not rigorous in theory. This paper is aim to establish a Mindlin plate element which can pass the strict constant shear patch test.

Three milestones have been gone through the development of patch test. Firstly, Bazeley *et al.* (1965) proposed the patch test for nonconforming element. It is the most practical method for testing the convergence of finite element which based on numerical calculation. However, it is not rigorous mathematically. Researchers have been investigating the theory of the patch test with the consideration of the effectiveness and practical applications. A mathematical description of the patch test was given by Strang (1972). Later, this description was explained as a constraint for single element, called individual element condition (Taylor *et al.* 1986) and can be used to construct element function. However, there is no rigorous mathematical proof for this patch test.

Secondly, based on rigorous mathematical theory, Stummel (1979) established a necessary and sufficient condition for the convergence of nonconforming element In addition, he had doubts about the patch test of Irons by proposing a simple approximation by nonconforming finite elements that passes the patch test of Irons but does not yield approximate solutions converging to the solution of the given boundary value problem (Stummel 1980). It should be noted that this rigorous convergence condition is for the whole problem domain not for an individual element, and the application of this condition requires a strong base of the functional analysis, which restrict its application to majority elements and the construction of nonconforming element. The development of finite element method necessitates that the patch test become a practical convergence criterion to be used not only to exam the element convergence but also as a guidance to construct the converged element. Although it is difficult to investigate the patch test mathematically, the patch test has long been used in engineering applications. Mathematical examples, which pass the patch test but fail to converge, generated considerable controversial opinions among engineering researchers (Taylor *et al.* 1986, Zienkiewicz *et al.* 1997).

Thirdly, Wang (2001) elucidated that besides the previously suggested requirements, the necessary and sufficient condition for patch test to be used as a convergence criterion should include the element function satisfying both theories of weak super-approximation and weak continuity. Wang's work pointed out that the example in Ref. (Stummel 1980) couldn't satisfy the two conditions and might clarify the uncertainty for patch test.

Historically, the displacement-based approach was the first attempt in the formulation of effective Reissner-Mindlin plate-bending elements. However, the original displacement element tends to cause the shear locking phenomenon which induces over-stiffness as the plate becomes progressively thinner for low order interpolation polynomials in the Reissner-Mindlin elements. The evaluation of the shear locking phenomenon has relied on numerical computations on thin plate problem. It is well known that the methods of reduced integration (Zienkiewicz *et al.* 1971) and selective integration (Hughes *et al.* 1978) are efficient approaches to prevent the appearance of the shear locking phenomenon. However, it is found that such elements often exhibit extra zero energy modes, and also produce oscillatory results for some problems. Moreover, it cannot pass the patch test for the analysis of very thin plates.

To overcome these deficiencies, stabilized techniques have been developed by author MacNeal (1978). Then subsequently, Belytschko *et al.* (1983) proposed the stabilization procedure to remove the zero-energy modes by perturbing the stiffness. Bathe and Dvorkin (1985) discussed a four-node plate bending element which had no lock and didn't contain any spurious zero energy modes.In addition, several efficient discrete shear elements based on the discrete Kirchhoff

constraint and the equilibrium conditions were developed by Batoz and Lardeur (1989), Batoz and Katili (1992), Katile (1993). These elements can eliminate locking phenomenon and converge towards the discrete Kirchhoff plate bending elements when the thickness of the plate is very thin. On the other hand, no element is free of shear locking in theory.

Bathe *et al.* (2000) introduced the MITC element and proposed strain energy patch test function to evaluate the convergence. Based on Timoshenko beam function, Soh *et al.* (1999) proposed a triangular 9 DOF plate bending element which can be employed to analyze very thin plate (the thickness/span ratio of the plate is about 10^{-11}). Soon, Soh *et al.* (2001) introduced a quadrilateral 12 DOF plate bending element. At this point, the progressively thinner plate which has the thickness/span ratio10^{-20} can be calculated. Chen and Cheung (2000) proposed the function of patch test for zero shear locking: $w=c_0+a_0x+b_0y+a_1x^2/2+c_1xy+b_2y^2/2$, $\theta_x=a_0+a_1x+c_1y$, $\theta_y=b_0+c_1x+b_1y$, a_i, b_i, c_i are arbitrary constants. It is apparent that this patch test is more rigorous than the patch test using numerical computation of pure bending and pure torsion of a small-scale plate. Then, the proposition of rectangular element RDKQM and triangular element RDKTM which can pass the above patch test functions (Chen and Cheung 2000, 2001) indicates that the shear locking problem is solved. Cen *et al.* (2006) established a quadrilateral element AC-MQ4 which employed the Timoshenko beam function and quadrilateral area coordinate. All the three elements RDKQM, RDKTM, and AC-MQ4 can be used to solve the extremely thin plate problem (the thickness/span ratio of the plate can reach to10^{-30}). In other words, these element solutions can accurately converge to thin plate finite element solutions.

On the other hand, mixed/hybrid stress elements (or assumed stress element) were also introduced to circumvent the difficulties outlined above. In particular, after the work of Malkus and Hughes (1978) on the equivalence between reduced integration displacements and mixed/hybrid stress models, this kind of approach became very useful in recent decades. Numerous effective elements have been proposed and employed by many authors, such as Lee and Pian (1978), Bathe and Dvorkin (1986), Sze and Chow (1991), Zienkiewicz *et al.* (1993), Taylor and Auricchio (1994), the MiSP family by Ayad *et al.* (1998), Cen *et al.* (2014) etc.

Due to the continuity conditions in inter-element, such as C^0 continuity of 2D/3D elasticity problems, C^1 continuity of thin plate problems and so on, the finite element trail function is defined in the Sobolev space which is also called generalized derivative space. There is not any particular external loading in the convergence theory in the Sobolev space. In terms of the variational basis of patch test proposed by Chen (2006), the test function for the patch test should satisfy the equilibrium equations without applied force yet. Chen (2006) proposed the enhanced patch test which can be applied to both homogeneous and inhomogeneous differential equations. Chen *et al.* (2009) proposed the enhanced patch test function for Mindlin plate. Current patch test for Mindlin plate only satisfies the zero shear deformation condition. The patch test of non-zero constant shear for Mindlin plate problem cannot be performed. The question of the convergence remained unresolved as to whether Mindlin plate can pass the non-zero constant shear stress patch test. Note that there was misunderstanding on this question. For example, Zhang and Kuang (2007) used the following patch test function $w=(x+y)/2$, $\theta_x=1/2$, $\theta_y=1/2$ to derive mistakenly $\gamma_{xz}=\partial w/\partial x-\theta_x=1$ and $\gamma_{yz}=\partial w/\partial y-\theta_y=1$, then drew the conclusion that the element passed the patch test of non-zero constant shear deformation. However, in fact, the above patch test is only for zero shear deformation. This example indicates the difficulty and lack of understanding to this question. Finally, the convergence test should be performed during the process of developing finite element method. Only pass the rigorous non-zero constant shear stress patch test, the convergence can be completely guaranteed.

Recently, different from the classical Timoshenko beam function, Jelenic and Papa (2011) proposed a new arbitrary order Timoshenko beam function. It's so far the only function which can be used to construct the functions of non-zero constant shear patch test for thick beam element. Since beam function can be regarded as a function on the boundary, the adopted hybrid stress method just requires the boundary function rather than the domain function. Because of this beam function is arbitrary order, thus it has high enough order to perform the non-zero constant shear stress patch test. Since it is required a complete cubic polynomial for the element function to pass the constant shear stress patch test. An 8-node quadrilateral assumed stress hybrid element is adopted.

The present work directly chooses the arbitrary order Timoshenko beam function as boundary displacement interpolation function. The purpose of this paper is to set up a quadrilateral Mindlin plate-bending finite element within an assumed stress formulation, whose main feature is that passes the rigorous enhanced non-zero constant shear patch test. To achieve this objective, the following steps have been taken. The first step concerns the choice of the variational framework with the adoption of complementary energy principle. Then the arbitrary order Timoshenko beam function as boundary displacement interpolation function is chosen for the proposed element. Since the choice of the stress approximation is a crucial issue in developing reliable hybrid finite element, selecting a suitable stress approximation which satisfies the plate equilibrium equations is not trivial. In order to improve the performance of the constructed element, a stress approximation ruled by 39 parameters is finally derived.

2. Enhanced patch test of finite element methods

The functional of the Hu-Washizu variational principle with relaxed inter-element continuity requirement in elasticity is given by

$$\pi_{mp} = \sum_{e=1}^{n} (\int_{V_e} ((\frac{1}{2}(F^T\mathbf{u}+\boldsymbol{\varepsilon})^T\mathbf{D}(F^T\mathbf{u}+\boldsymbol{\varepsilon})-\boldsymbol{\sigma}^T\boldsymbol{\varepsilon})dv - \int_{\partial V_e} \boldsymbol{\sigma}^T\mathbf{R}^T(\mathbf{u}-\tilde{\mathbf{u}})ds) - W \tag{1}$$

where $\mathbf{u}$ is the element displacement without inter-element continuity requirement and $\tilde{\mathbf{u}}$ is the element boundary displacement expressed in terms of nodal displacements, which contain the rigid body and the constant strain modes; n is the number of elements; $\boldsymbol{\varepsilon}$, $\boldsymbol{\sigma}$ are the constant strain and constant stress, respectively; F^T is the strain differential operator; $\mathbf{D}$ is the matrix of elasticity constants; the boundary force $\mathbf{T}$ corresponding to the constant stress is given by $\mathbf{T}=\mathbf{R}\boldsymbol{\sigma}$; $\mathbf{R}$ is the matrix of the direction cosines of the element boundary; and W is the work of the external force. Based on this variational principle, Chen *et al*. (1987, 1998) established a series of generalized hybrid element.

Chen and Cheung (1996, 1997) proposed a refined non-conforming variational principle. For the non-conforming element displacement $\mathbf{u}$ and the boundary displacement $\tilde{\mathbf{u}}$ which are expressed in terms of nodal displacements and contain the rigid body and the constant strain modes, the functional of variational principle for non-conforming element is given as

$$\pi_{mp}^* = \sum_{e=1}^{n} (\int_{V_e} ((\frac{1}{2}(F^T\mathbf{u}+\boldsymbol{\varepsilon}_c)^T\mathbf{D}(F^T\mathbf{u}+\boldsymbol{\varepsilon}_c)-\boldsymbol{\sigma}_c^T\boldsymbol{\varepsilon}_c)dv - \int_{\partial V_e} \boldsymbol{\sigma}_c^T\mathbf{R}_c^T(\mathbf{u}-\tilde{\mathbf{u}})ds) - W \tag{2}$$

where $\boldsymbol{\varepsilon}_c$, $\boldsymbol{\sigma}_c$ are the constant strain and constant stress, respectively; the boundary force $\mathbf{T}_c$

corresponding to the constant stress is given by $\mathbf{T}_c = \mathbf{R}\boldsymbol{\sigma}_c$.

By using $\delta\pi_{mp}^* = 0$, we obtain the individual element condition of the patch test

$$\int_{V_e} \boldsymbol{\sigma}_c^T F^T \mathbf{u}^* dv = \int_{\partial V_e} \mathbf{T}_c^T \tilde{\mathbf{u}} ds \qquad (3)$$

where $\mathbf{u}^*$ is the element displacement function, which can be either conforming or nonconforming, $\tilde{\mathbf{u}}$ is inter-element boundary displacement function. For conforming element, $\tilde{\mathbf{u}}$ is the value of element displacement at the boundary. For nonconforming element, $\tilde{\mathbf{u}}$ is independent of element displacement $\mathbf{u}$. $\boldsymbol{\sigma}_c$ is the constant stress that satisfies the equilibrium equation, $\mathbf{T}_c$ is the boundary force. It can be proved that the individual element condition is the sufficient condition for passing the constant stress patch test of homogeneous differential equations Taylor *et al* (1986).

For inhomogeneous differential equations, Chen (2006) proposed a new variational principle functional for non-conforming element which can be given by

$$\pi_{mp}^* = \sum_{e=1}^{n} (\int_{V_e} (\frac{1}{2}(F^T\mathbf{u} + \mathbf{N}\boldsymbol{\alpha})^T \mathbf{D}(F^T\mathbf{u} + \mathbf{N}\boldsymbol{\alpha}) - \boldsymbol{\beta}^T \mathbf{P}^T \mathbf{N}\boldsymbol{\alpha}) dv - \int_{\partial V_e} \mathbf{T}_a^T (\mathbf{u} - \tilde{\mathbf{u}}) ds) - W \qquad (4)$$

where $\mathbf{N}\boldsymbol{\alpha}$, $\mathbf{P}\boldsymbol{\beta}$ are the special strain and special stress, respectively; $\mathbf{N}$ is interpolation matrix; the boundary force $\mathbf{T}_a$ corresponding to the special stress is given by $\mathbf{T}_a = \mathbf{R}\mathbf{P}\boldsymbol{\beta}$.

By using $\delta\pi_{mp}^* = 0$, we obtain the individual element condition of the patch test

$$\int_{V_e} \boldsymbol{\sigma}_a^T F^T \mathbf{u}^* dv = \int_{\partial V_e} \mathbf{T}_a^T \tilde{\mathbf{u}} ds - \int_{V_e} \left(F_s\boldsymbol{\sigma}_a^T\right)\mathbf{u} dv \qquad (5)$$

where $\boldsymbol{\sigma}_a$ is the stress of the element that satisfies the equilibrium equation which without external force, $\boldsymbol{\sigma}_a$ contains the constant stress and non-constant stress. It can be proved that the individual element condition is the sufficient condition for passing the patch test of inhomogeneous differential equations (Chen 2006).

The convergence criterion requires that besides passing the enhanced patch test, the element function should include the rigid body modes and the lowest order non-zero strain modes of the equilibrium state (or fundamental strain mode), and no spurious zero energy modes occur.

In the case of the inhomogeneous differential equation, the lowest order stress term is chosen to be non-zero constant stress. The other stresses determined from the inhomogeneous differential equation cannot be constant. Therefore, the compatibility condition of the element function will be more rigorous. In the case of homogeneous differential equation, the constant stress satisfies the equilibrium equation automatically, and the enhanced patch test degenerates into the constant stress patch test automatically. Therefore, the enhanced patch test is applicable to both homogeneous and inhomogeneous differential equations.

3. The arbitrary order Timoshenko beam function

Euler-Bernoulli beam function has been successfully employed in the construction of refined thin plate elements. It is well known that when constructing Mindlin plate element, both thick and thin plates should be taken into account, and it is necessary to eliminate shear locking phenomenon. To seek out such element displacement function is definitely very difficult. Note that

a closed form solution for both thick and thin beams exists in the form of the Timoshenko beam function, and it is possible to use it to derive more efficient Mindlin plate elements (Soh *et al*. 1999). However, the use of Timoshenko beam function is capable of solving the problem of shear locking, it cannot solve the problem of passing the non-zero constant shear patch test. This problem hasn't been resolved for many years. Recently, Jelenic and Papa (2011) presented a new arbitrary order Timoshenko beam function. This is the only function which can be used to construct the functions of non-zero constant shear patch test for thick beam element so far. The arbitrary order Timoshenko beam function can be given as follows

$$w = \sum_{i=1}^{n} I_i w_i - \frac{L}{n} \prod_{j=1}^{n} N_j \sum_{i=1}^{n} (-1)^{i-1} \binom{n-1}{i-1} \theta_i, \quad \theta = \sum_{i=1}^{n} I_i \theta_i \tag{6}$$

where L is the beam length, w_i and θ_i are the values of the displacements and the rotations at the n nodes equidistantly spaced between the beam ends, I_i are the standard Lagrange polynomials of order $n-1$, and $N_j = x/L$ for $j=1$ and $N_j = 1-(n-1)/(j-1)(x/L)$ otherwise, in which x is the coordinate along the beam.

4. Fundamental equations of Mindlin plate

Consider a plate referred to a Cartesian coordinate frame (o,x,y,z), with the origin o on the mid-surface Ω and the z-axis in the thickness direction, $-h/2 \leq z \leq h/2$, where h is the plate thickness. Let $\partial\Omega$ be the boundary of Ω. The Reissner-Mindlin theory, i.e., the first-order shear deformable theory, is employed. Thus it is assumed that

$$u(x,y,z) = z\theta_y, \quad v(x,y,z) = -z\theta_x, \quad w(x,y,z) = w(x,y) \tag{7}$$

where u, v, w are displacements along the x, y and z axes, respectively, and θ_x, θ_y are the rotations of the transverse normal about the x and y axes, w is the transverse displacement field.

The geometric equations can be written as follows

$$\boldsymbol{\chi} = \mathbf{B}_b \boldsymbol{\theta}, \quad \boldsymbol{\gamma} = \mathbf{B}_s w + \hat{\mathbf{I}}\boldsymbol{\theta} \tag{8}$$

where $\boldsymbol{\theta} = [\theta_x \; \theta_y]^T$, $\boldsymbol{\chi} = [\chi_x \; \chi_y \; \chi_{xy}]^T$ and $\boldsymbol{\gamma} = [\gamma_{xz} \; \gamma_{yz}]^T$ respectively, the rotations, the curvatures and the shear strains and operators $\mathbf{B}_b = \begin{bmatrix} 0 & \partial/\partial x \\ -\partial/\partial y & 0 \\ -\partial/\partial x & \partial/\partial y \end{bmatrix}, \mathbf{B}_s = \begin{bmatrix} \partial/\partial x \\ \partial/\partial y \end{bmatrix}, \hat{\mathbf{I}} = \begin{bmatrix} 0 & 1 \\ -1 & 0 \end{bmatrix}$

The equilibrium equations can be obtained from the strain energy in the form

$$-\mathbf{B}_b^T \mathbf{M} + \hat{\mathbf{I}}^T \mathbf{S} = \mathbf{0}, \quad \mathbf{B}_s^T \mathbf{S} = \mathbf{0} \tag{9}$$

where vectors $\mathbf{M} = [M_x \; M_y \; M_{xy}]^T$ and $\mathbf{S} = [S_x \; S_y]^T$, respectively, the moment and shear resultants. The boundary forces can be written as follows

$$\mathbf{T} = \begin{bmatrix} 0 & -\sin\alpha & -\cos\alpha & 0 & 0 \\ \cos\alpha & 0 & \sin\alpha & 0 & 0 \\ 0 & 0 & 0 & \cos\alpha & \sin\alpha \end{bmatrix} \begin{bmatrix} \mathbf{M} \\ \mathbf{S} \end{bmatrix} = \mathbf{R} \begin{bmatrix} \mathbf{M} \\ \mathbf{S} \end{bmatrix} \tag{10}$$

where α is the angle between the normal of edge and the local x-axis of element.

For a linearly elastic material, the constitutive equations can be written as

$$\mathbf{M} = \mathbf{D}_b \mathbf{\chi}, \quad \mathbf{S} = \mathbf{D}_s \mathbf{\gamma} \tag{11}$$

where $\mathbf{D}_b = \dfrac{Eh^3}{12\left(1-\mu^2\right)} \begin{bmatrix} 1 & \mu & 0 \\ \mu & 1 & 0 \\ 0 & 0 & \dfrac{1-\mu}{2} \end{bmatrix}$ and $\mathbf{D}_s = kGh \begin{bmatrix} 1 & 0 \\ 0 & 1 \end{bmatrix}$ are the elasticity matrices of bending

and transverse shear moduli, being E the Young's modulus, G the shear modulus, μ the Poisson's ration, and $k=5/6$ a correction factor to account for non-uniform distribution of shear stresses through the thickness.

Substituting geometric Eq. (8) and stress-strain relation (11) into the equilibrium Eq. (9), the equilibrium equations are obtained in terms of displacements

$$\begin{cases} \dfrac{Eh^3}{12\left(1-\mu^2\right)}\left(\dfrac{\partial^2\theta_y}{\partial x^2} + \dfrac{1-\mu}{2}\dfrac{\partial^2\theta_y}{\partial y^2} - \dfrac{1+\mu}{2}\dfrac{\partial^2\theta_x}{\partial x\partial y}\right) - kGh\left(\dfrac{\partial w}{\partial x} + \theta_y\right) = 0 \\[2mm] \dfrac{Eh^3}{12\left(1-\mu^2\right)}\left(\dfrac{1+\mu}{2}\dfrac{\partial^2\theta_y}{\partial x\partial y} - \dfrac{\partial^2\theta_x}{\partial y^2} - \dfrac{1-\mu}{2}\dfrac{\partial^2\theta_x}{\partial x^2}\right) - kGh\left(\dfrac{\partial w}{\partial y} - \theta_x\right) = 0 \\[2mm] kGh\left(\dfrac{\partial^2 w}{\partial x^2} + \dfrac{\partial^2 w}{\partial y^2} + \dfrac{\partial\theta_y}{\partial x} - \dfrac{\partial\theta_x}{\partial y}\right) = 0 \end{cases} \tag{12}$$

In the patch test, the test function should satisfy the equilibrium Eq. (12).

5. Formulation of 24-DOF hybrid stress Mindlin plate element

5.1 Assumed stress Hybrid formulation

The element developed in this paper is based on complementary energy principle. The complementary energy principle can be written as

$$\Pi_e = \int_{\Omega_e} \frac{1}{2}\boldsymbol{\sigma}^T\mathbf{D}^{-1}\boldsymbol{\sigma}d\Omega - \int_{\partial\Omega_e} \mathbf{T}^T\overline{\mathbf{u}}dS \tag{13}$$

where $\boldsymbol{\sigma}$ is the stress vector, $\mathbf{D}$ is the elasticity matrices, $\mathbf{T}$ is the vector of boundary force, and $\overline{\mathbf{u}} = \begin{bmatrix} \tilde{w} & \tilde{\theta}_x & \tilde{\theta}_y \end{bmatrix}^T$ is the boundary displacement vector, and $\tilde{w}$ is the transverse displacement, $\tilde{\theta}_x, \tilde{\theta}_y$ are the rotations of the transverse normal about the x and y axes.

The approximation for stress and boundary displacements can now be incorporated in the functional. The stress field is described in the interior of the element as

$$\begin{bmatrix} M_x & M_y & M_{xy} & S_x & S_y \end{bmatrix}^T = \mathbf{P}\boldsymbol{\beta} \tag{14}$$

where $\mathbf{P}$ is matrix of stress interpolation functions, and $\boldsymbol{\beta}$ is the unknown stress parameters.

The boundary force $\mathbf{T}$ can be represented as

$$\mathbf{T} = \mathbf{RP}\boldsymbol{\beta} \tag{15}$$

where $\mathbf{R}$ is the combination of direction cosine for the boundary normal.

The boundary displacement field is described by

$$\bar{\mathbf{u}} = \begin{bmatrix} \tilde{w} & \tilde{\theta}_x & \tilde{\theta}_y \end{bmatrix}^T = \mathbf{Lq} \tag{16}$$

where $\mathbf{L}$ are interpolation functions, $\mathbf{q}$ is nodal displacement parameters.

Substituting the stress Eq. (14), boundary force Eq. (15) and displacement approximations Eq. (16) into the functional (13)

$$\Pi_e = \frac{1}{2}\boldsymbol{\beta}^T \mathbf{H}\boldsymbol{\beta} - \boldsymbol{\beta}^T \mathbf{Gq} \tag{17}$$

where

$$\mathbf{H} = \int_{\Omega_e} \mathbf{P}^T \mathbf{D}^{-1} \mathbf{P} d\Omega \tag{18}$$

$$\mathbf{G} = \int_{\partial\Omega_e} (\mathbf{RP})^T \mathbf{L} dS \tag{19}$$

The form of Eqs. (18) and (19) is directly amenable to numerical integration (i.e., Gauss quadrature). In principle, integration rules should be chosen which integrate all terms in $\mathbf{H}$ and $\mathbf{G}$ exactly. Then the internal strain energy can be expressed as

$$U = \int_{\Omega_e} \frac{1}{2}\boldsymbol{\sigma}^T \mathbf{D}^{-1}\boldsymbol{\sigma} d\Omega = \frac{1}{2}\boldsymbol{\beta}^T \mathbf{H}\boldsymbol{\beta} \tag{20}$$

By means of $\partial \Pi_e/\partial\boldsymbol{\beta}=0$, we obtained

$$\mathbf{H}\boldsymbol{\beta} = \mathbf{Gq} \tag{21}$$

consequently

$$\boldsymbol{\beta} = \mathbf{H}^{-1}\mathbf{Gq} \tag{22}$$

Substitution of $\boldsymbol{\beta}$ in Eq. (20), the internal strain energy reduces to

$$U = \mathbf{q}^T \mathbf{G}^T \mathbf{H}^{-1} \mathbf{Gq}/2 \tag{23}$$

Compared with $U=(1/2)\mathbf{q}^T\mathbf{Kq}$, the element stiffness matrix can be taken as

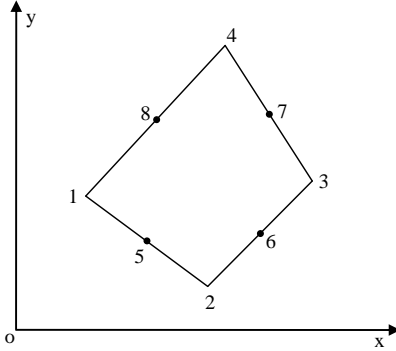$$\mathbf{K} = \mathbf{G}^T \mathbf{H}^{-1} \mathbf{G} \tag{24}$$

Fig. 1 Eight-node quadrilateral plate element   Fig. 2 Quadrilateral element's 1-2 boundary
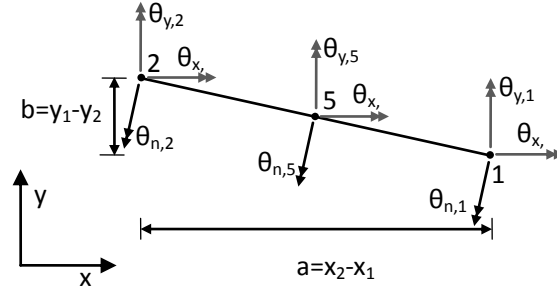
The solution of the system yields the unknown nodal displacements $\mathbf{q}$. After $\mathbf{q}$ is determined, element stress or internal forces can be recovered by use of Eqs. (22) and (14). Thus

$$\boldsymbol{\sigma} = \mathbf{P}\mathbf{H}^{-1}\mathbf{G}\mathbf{q} \tag{25}$$

In modeling structures using displacement based or hybrid elements, body forces applied to the elements are replaced by equivalent nodal forces. With this replacement, the stiffness and stress matrices in element formulations need only to be considered for forces applied at the nodes.

5.2 Formulation of 24-DOF hybrid stress Mindlin plate element

5.2.1 Boundary displacement interpolation based on arbitrary order Timoshenko beam function

As mentioned above, the main drawback of low-order Mindlin plate element is incapable of passing the non-zero constant shear patch test. The introduction of arbitrary order Timoshenko beam function can avoid this problem. Since beam function is arbitrary order and functions of arbitrary order can be obtained, if the order is improved then it can be used to do the non-zero constant shear stress patch test. In order to pass strict constant shear stress patch test, a complete cubic polynomial is required, thus an 8-node quadrilateral assumed stress hybrid element is adopted. According to this idea, an 8-node quadrilateral element was designed as given in Fig. 1. If any quadrilateral side is taken as a beam element, take the 1-2 boundary as example.

$(L^2 = a^2 + b^2)$ is the length of 1-2 boundary, the displacement $\tilde{w}$ can be derived, with node 5 located at the middle of the side as show in Fig. 2.

$$
\begin{aligned}
\tilde{w} &= I_1 w_1 + I_2 w_2 + I_5 w_5 - I_0 L \left(-\theta_{n,1} + 2\theta_{n,5} - \theta_{n,2} \right) \\
&= I_1 w_1 + I_2 w_2 + I_5 w_5 - I_0 \left[\left(-\theta_{x,1} + 2\theta_{x,5} - \theta_{x,2} \right) b + \left(-\theta_{y,1} + 2\theta_{y,5} - \theta_{y,2} \right) a \right] \\
\tilde{\theta}_x &= I_1 \theta_{x,1} + I_2 \theta_{x,2} + I_5 \theta_{x,5}, \quad \tilde{\theta}_y = I_1 \theta_{y,1} + I_2 \theta_{y,2} + I_5 \theta_{y,5}
\end{aligned} \tag{26}
$$

where $I_1 = L_1(2L_1 - 1)$, $I_2 = L_2(2L_2 - 1)$, $I_5 = 4L_1 L_2$, $I_0 = L_1 L_2(L_2 - L_1)/3$, $L_1 = 1 - s/L$, $L_2 = s/L$, and s is the coordinate along the 1-2 edge.

The displacement components $\bar{\mathbf{u}}$ along the 1-2 boundary was given as follows

$$\bar{\mathbf{u}}_{1\text{-}2} = \begin{bmatrix} \tilde{w} & \tilde{\theta}_x & \tilde{\theta}_y \end{bmatrix}^T = \begin{bmatrix} I_1 & I_0 b & I_0 a & I_2 & I_0 b & I_0 a & I_5 & -2I_0 b & -2I_0 a \\ 0 & I_1 & 0 & 0 & I_2 & 0 & 0 & I_5 & 0 \\ 0 & 0 & I_1 & 0 & 0 & I_2 & 0 & 0 & I_5 \end{bmatrix} \mathbf{q}_{1\text{-}2} = \mathbf{L}_{1\text{-}2}\mathbf{q}_{1\text{-}2} \quad (27)$$

where $\mathbf{q}_{1\text{-}2}=[\mathbf{q}_1\ \mathbf{q}_2\ \mathbf{q}_5]^T$, $\mathbf{q}_i=[w_i\ \theta_{xi}\ \theta_{yi}]^T$ (i=1,2,5).

5.2.2 Assumed stresses

In this section, a strategy to select the stress approximation in a rational way is presented. Note that the stress functions should satisfy the equilibrium Eq. (9). In practice, initial polynomials are usually assumed for the stresses after which the equilibrium equations are applied to these polynomials yielding relations between the β's and ultimately the final form of $\mathbf{P}$. The number of stress parameters, which is the number of columns in $\mathbf{P}$, must be at least equal to the number of degrees of freedom of the element less the number of degrees of freedom necessary to prevent rigid body motion. The following equilibrating stress resultant field is considered.

$$\begin{bmatrix} M_x & M_y & M_{xy} & S_x & S_y \end{bmatrix}^T = \mathbf{P}\boldsymbol{\beta} \tag{28}$$

where $\boldsymbol{\beta}=\{\beta_i\}$, i=1,...,N_b.

Conventional choice of $\mathbf{P}\boldsymbol{\beta}$ is $N_b(\boldsymbol{\beta})\geq n_\mathbf{q}-n_\mathrm{r}$, while the optimal selection is $N_b(\boldsymbol{\beta})=n_\mathbf{q}-n_\mathrm{r}$, $n_\mathbf{q}$ and n_r being the degrees of freedom of the element and the number of allowed rigid body motions, respectively. The element has 24-DOF, therefore, a stress field with at least 21 parameters is needed to describe the stress field and without spurious zero energy modes. Firstly the number of $\{\beta_i\}$ is chosen as N_b=21 (the first 21 stress functions in Table 1). Numerical results show that the

Table 1 Assumed stress function (i=1…N_b)

i	1	2	3	4	5	6	7	8	9	10	11	12	13	14	15	16	17
M_x	1	0	0	x	y	0	0	0	0	x^2	xy	y^2	0	0	0	0	0
M_y	0	1	0	0	0	x	y	0	0	0	0	0	x^2	xy	y^2	0	0
M_{xy}	0	0	1	0	0	0	0	x	y	$-xy$	0	0	0	0	$-xy$	x^2	y^2
Q_x	0	0	0	1	0	0	0	0	1	x	y	0	0	0	$-x$	0	$2y$
Q_y	0	0	0	0	0	0	1	1	0	$-y$	0	0	0	x	y	$2x$	0

i	18	19	20	21	22	23	24	25	26	27	28	29
M_x	x^3	x^2y	xy^2	y^3	0	0	0	0	0	0	x^4	x^3y
M_y	0	0	0	0	x^3	x^2y	xy^2	y^3	0	0	$-6x^2y^2$	0
M_{xy}	$-1.5x^2y$	$-0.5xy^2$	0	0	0	0	$-0.5x^2y$	$-1.5xy^2$	x^3	y^3	0	$-0.75x^2y^2$
Q_x	$1.5x^2$	xy	y^2	0	0	0	$-0.5x^2$	$-3xy$	0	$3y^2$	$4x^3$	$1.5x^2y$
Q_y	$-3xy$	$-0.5y^2$	0	0	0	x^2	xy	$1.5y^2$	$3x^2$	0	$-12x^2y$	$-1.5xy^2$

i	30	31	32	33	34	35	36	37	38	39
M_x	xy^3	y^4	0	0	0	$-6x^2y^2$	0	0	$-3x^2y^2$	0
M_y	0	0	x^4	x^3y	xy^3	y^4	0	$-3x^2y^2$	0	0
M_{xy}	0	0	0	0	$-0.75x^2y^2$	0	x^4	x^3y	xy^3	y^4
Q_x	y^3	0	0	0	$-1.5x^2y$	$-12xy^2$	0	x^3	$-3xy^2$	$4y^3$
Q_y	0	0	0	x^3	$1.5xy^2$	$4y^3$	$4x^3$	$-3x^2y$	y^3	0

stiffness matrix has two Spurious zero energy modes (list in Table 6) and converges slowly (list in Table 7). The study find that gradually increasing the number of $\{\beta_i\}$ until $N_b=28$ (fourth order), there is a proper rank for the stiffness matrix and the absence of spurious zero energy modes (list in Table 6). Moreover, the calculation results are accurate and converged faster. And they are better if the number of $\{\beta_i\}$ reaches $N_b=39$ (complete quartic polynomial). Numerical experimentations indicate that this 39 parameter selection of stress field is somewhat more accurate and has no spurious zero energy modes (list in Table 6). For this reason, 39β are chosen as the assumed stress field.

It can be shown that the above approximation satisfies the equilibrium Eq. (9). From Eq. (10) the boundary force **T** can be expressed as

$$\mathbf{T} = \mathbf{RP\beta} \tag{29}$$

Then, along the boundary 1-2, **G** can be obtained

$$\mathbf{G}_{12} = \int_{\partial\Omega(1-2)} (\mathbf{RP})^T \mathbf{L}_{1-2} \, ds \tag{30}$$

Similarly, along the other boundaries, $\mathbf{G}_{23}$, $\mathbf{G}_{34}$, $\mathbf{G}_{41}$ can also be obtained by cyclic permutation.

6. The function of patch test for Mindlin plate element

According to the equilibrium equations, if the stress terms M_x, M_y, M_{xy} are constants, then S_x and S_y equal to zero. In this case, it passes the constant bending moment patch test. With the purpose of passing the non-zero constant shear deformation patch test, the order of the stress terms M_x, M_y, M_{xy} in the non-homogeneous equations has to be equal or greater than 1. This requires the displacement functions θ_x, θ_y to pass the linear bending moment patch test. $\gamma_{zx}=\partial w/\partial x+\theta_y$ and $\gamma_{yz}=\partial w/\partial y-\theta_x$ are arbitrary non-zero constant strains. The function w is one order higher than the order of displacement functions θ_x, θ_y.

The elements developed by Chen and Cheung (2000, 2001) can pass the zero shear patch test. For zero shear deformation patch test, θ_x and θ_y are linear functions, w is quadratic function. They can be assumed as follows

$$\begin{cases} w = a_0 + a_1 x + a_2 y + a_3 x^2 + a_4 xy + a_5 y^2 \\ \theta_x = b_0 + b_1 x + b_2 y \\ \theta_y = c_0 + c_1 x + c_2 y \end{cases} \tag{31}$$

where a_i, $(i=0...5)$, b_0, b_1, b_2, c_0, c_1, c_2, are arbitrary constants.

Due to the test function should satisfy the equilibrium equations in terms of displacements, substituting Eq. (31) into equilibrium Eq. (12), the test functions can be obtained as follows

$$\begin{cases} w = a_0 + a_1 x + a_2 y + a_3 x^2 + a_4 xy + a_5 y^2 \\ \theta_x = a_2 + a_4 x + 2a_5 y \\ \theta_y = -a_1 - 2a_3 x - a_4 y \end{cases} \tag{32}$$

For non-zero constant shear deformation patch test, θ_x and θ_y are quadratic functions, w is cubic

equation. They can be expressed as

$$\begin{cases} w = a_0 + a_1 x + a_2 y + a_3 x^2 + a_4 xy + a_5 y^2 + a_6 x^3 + a_7 x^2 y + a_8 xy^2 + a_9 y^3 \\ \theta_x = b_0 + b_1 x + b_2 y + b_3 x^2 + b_4 xy + b_5 y^2 \\ \theta_y = c_0 + c_1 x + c_2 y + c_3 x^2 + c_4 xy + c_5 y^2 \end{cases} \tag{33}$$

where a_i, $(i=0...9)$, b_i, $(i=0...5)$ and c_i, $(i=0...5)$ are arbitrary constants.

Due to the test function should satisfy the equilibrium equations in terms of displacements, substituting Eq. (33) into equilibrium Eq. (12), the test functions can be obtained as follows

$$\begin{cases} w = a_0 + a_1 x + a_2 y + a_3 x^2 + a_4 xy + a_5 y^2 + a_6 x^3 + a_7 x^2 y + a_8 xy^2 + a_9 y^3 \\ \theta_x = \dfrac{h^2}{3k(1-\mu)}(a_7 + 3a_9) + a_2 + a_4 x + 2a_5 y + a_7 x^2 + 2a_8 xy + 3a_9 y^2 \\ \theta_y = -\dfrac{h^2}{3k(1-\mu)}(3a_6 + a_8) - a_1 - 2a_3 x - a_4 y - 3a_6 x^2 - 2a_7 xy - a_8 y^2 \end{cases} \tag{34}$$

where a_i, $(i=0...9)$ are arbitrary constants.

7. Numerical test

In this section, the numerical study of the described elements, hereinafter called QH8-21β with $N_b=21$, QH8-28β with $N_b=28$ and QH8-39β with $N_b=39$ are numerically verified on some standard test problems including thin and thick plates and compared with that of other quadrilateral elements available in literature. Note that the present element QH8-39β is a high order element, each element has 8 nodes and 24 degrees of freedom. The other quadrilateral elements for comparison are 4 nodes element with 12 degrees of freedom. Obviously, when four nodes and eight nodes element are compared on the same mesh, the eight node element has higher computational cost. However, the eight nodes Mindlin plate element can pass the non-zero constant shear patch test, the four nodes element cannot. In fact, modern computers has high computational efficiency and high-speed processing of massive data. Although the QH8-39β element is somewhat time-consuming, it is acceptable to the modern computer.

7.1 Patch test: consistency assessment

Consistency of the developed elements is tested for the constant strain and stress states on the patch example with five elements, covering a rectangular domain of a plate as shown in Fig. 3. The size of the domain is 0.24×0.12. The mechanical properties of the plate are chosen as $E=10^3$, $\mu=0.25$, $k=5/6$. We tested the following states:

Constant bending state

In this test, the coefficients a_i, $(i=0...5)$ of the test functions in Eq. (32) are listed in Table 2. The displacements at the nodes on the boundaries are imposed according to Eq. (32). The exact displacements and rotations at the internal nodes are expected. The numerical results of the patch

Table 2 The coefficients of constant bending patch test functions

a_0	a_1	a_2	a_3	a_4	a_5
1	2	3	4	5	6

Table 3 Numerical results of constant bending patch test (at node 1)

	$h=1$					$h=0.01$				
	w	θ_x	θ_y	S_x	S_y	w	θ_x	θ_y	S_x	S_y
QH8-21β	1.1528	3.440	-2.420	0	0	1.1528	3.440	-2.420	0	0
QH8-39β	1.1528	3.440	-2.420	0	0	1.1528	3.440	-2.420	0	0
Exact	1.1528	3.440	-2.420	0	0	1.1528	3.440	-2.420	0	0

Table 4 The coefficients of non-zero constant stress patch test functions

a_0	a_1	a_2	a_3	a_4	a_5	a_6	a_7	a_8	a_9
1	2	3	4	5	6	7	8	9	10

Table 5 Numerical results of nonzero constant stress patch test (at node 1)

	$h=1$					$h=0.01$				
	w	θ_x	θ_y	S_x	S_y	w	θ_x	θ_y	S_x	S_y
QH8-21β	1.1537	23.7459	-18.470	-5333	-6756	1.1537	3.4812	-2.4716	-0.0053	-0.0068
QH8-39β	1.1537	23.7459	-18.470	-5333	-6756	1.1537	3.4812	-2.4716	-0.0053	-0.0068
Exact	1.1537	23.7459	-18.470	-5333	-6756	1.1537	3.4812	-2.4716	-0.0053	-0.0068

test at node 1 are listed in Table 3. The results demonstrate that both of the proposed hybrid stress elements QH8-21β and QH8-39β can pass the constant bending patch test with zero shear stresses S_x, S_y.

Non-zero constant shear state

In this test, the coefficients a_i, (i=0...9) of the test functions in Eq. (34) are listed in Table 4. The displacements at the nodes on the boundaries are imposed according to Eq. (34). The exact displacements and rotations at the internal nodes are expected. The numerical results of the patch test at node 1 are listed in Table 5. The results demonstrate that both of the proposed hybrid stress elements QH8-21β and QH8-39β can pass the strict patch test with non-zero constant shear stresses S_x, S_y.

The patch test mesh of hybrid stress quadrilateral element is presented in Fig. 3. Given the displacements and rotations at the boundary nodes (8 displacements and 16 rotations), while all the internal nodal displacements and rotations are to be calculated by the finite element solution procedure. Test results (Tables 3 and 5) show that the elements QH8-21β and QH8-39β can pass both the constant bending and non-zero constant shear test.

7.2 Stability assessment

As a test of stability, an eigenvalues analysis on the stiffness matrix for one regular element is performed. Table 6 reports the first six eigenvalues computed by the single QH8-21β element,
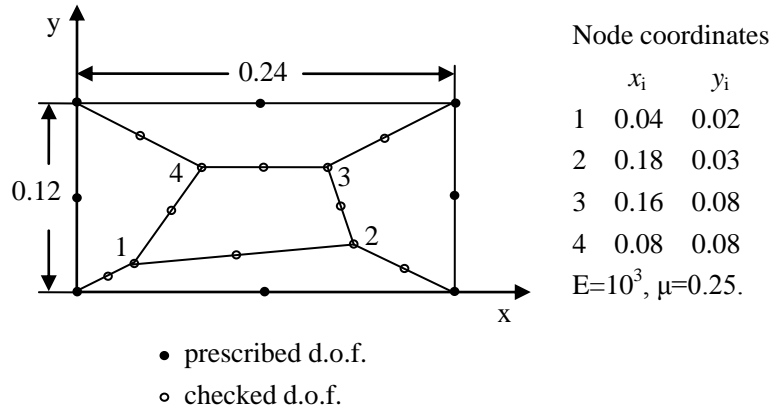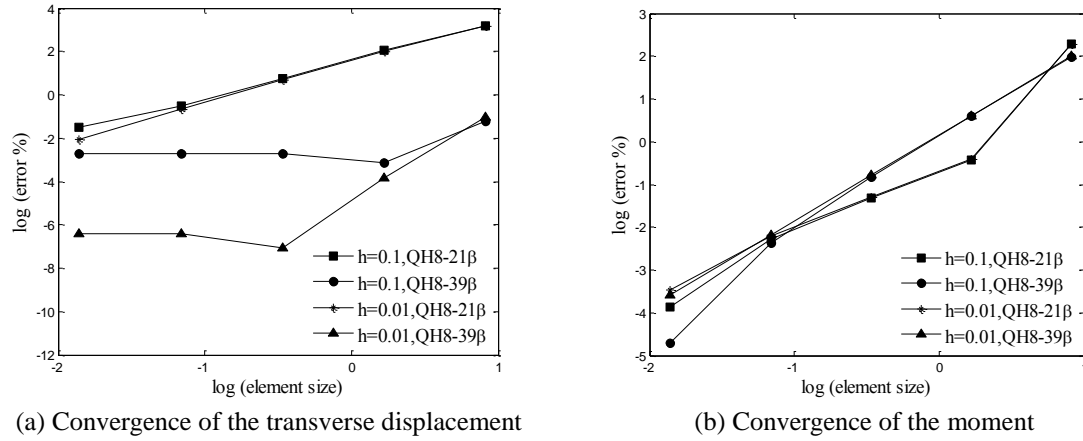
	Node coordinates
	x_i y_i
1	0.04 0.02
2	0.18 0.03
3	0.16 0.08
4	0.08 0.08
	$E=10^3$, $\mu=0.25$.

• prescribed d.o.f.

○ checked d.o.f.

Fig. 3 Element patch for consistency assessment of eight-node elements

Table 6 Eigenvalues for regular mesh

Element	QH8-21β	QH8-28β	QH8-39β
	3.7838e-16	-2.2237e-16	3.8340e-16
	5.8224e-16	-2.2237e-16	-5.2094e-16
Eigenvalue	-2.2450e-16	1.0640e-15	-5.2094e-16
	-2.2450e-16	0.0371	0.0371
	-5.3198e-16	0.0371	0.0371
	0.0130	0.0474	0.0363
Spurious zero energy modes	5-3=2	3-3=0	3-3=0
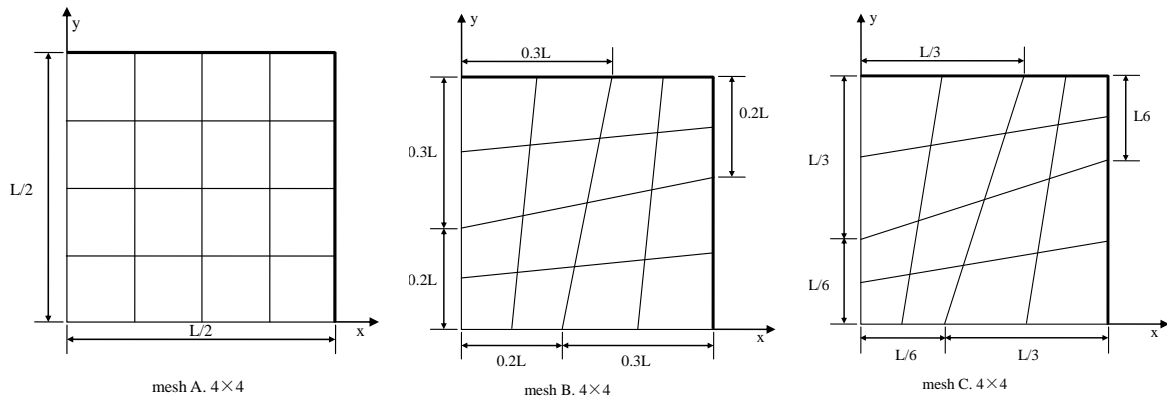
Fig. 4 Typical meshes (4×4) for square plate (mesh density *N*=4)

QH8-28β element and QH8-39β element, respectively. The following data are assumed: *E*=1000, μ=0.25, *h*=0.1. Two spurious modes are observed for the QH8-21β element. Then gradually increasing the number of $\{\beta_i\}$ until N_b=28, three zero eigenvalues corresponding to the three rigid body motions of a plate are obtained for the QH8-28β element, showing thus a proper rank for the stiffness matrix and the absence of spurious modes in consequence. The QH8-39β element has the same stability as the QH8-28β element.

(a) Convergence of the transverse displacement   (b) Convergence of the moment

Fig. 5 Performance of the elements QH8-21β and QH8-39β

Table 7 Comparison between the element QH8-21β and QH8-39β

Element mesh	h=0.1				h=0.01			
	QH8-21β		QH8-39β		QH8-21β		QH8-39β	
	w^*	M^*	w^*	M^*	w^*	M^*	w^*	M^*
1×1	0.0601	3.0098	0.1229	2.1528	0.0510	3.0118	0.1227	2.1511
2×2	0.0963	2.5163	0.1263	2.1226	0.0962	2.5182	0.1261	2.1208
4×4	0.1170	2.3055	0.1268	2.2490	0.1169	2.3057	0.1265	2.2484
8×8	0.1240	2.2843	0.1268	2.2805	0.1240	2.2842	0.1265	2.2801
16×16	0.1259	2.2881	0.1268	2.2883	0.1259	2.2880	0.1265	2.2879
32×32	0.1264	2.2900	0.1268	2.2903	0.1264	2.2898	0.1265	2.2899
exact	0.1267	2.2910			0.1265	2.2905		

7.3 Square plate under uniform load

Fig. 4 shows the typical meshes employed for the study of a square plate. Mesh A is the regular type, whereas mesh B and C are the distorted types and the mesh density N=4. Owing to the biaxial symmetry, only one-quarter of the plate is described. Moreover, a clamped ($w=\theta_x=\theta_y=0$) and a simply supported (SS2: displacements and rotations around the normal to the edge set to zero) cases were considered. The plate material properties are assumed: E=10.92, μ=0.3, k=5/6. The loading on the plate is uniformly distributed of magnitude q=1.

7.3.1 Numerical investigation on selection of β parameters

The performance of the element QH8-21β and QH8-39β are compared when h=0.1 and 0.01 (Mesh A in Fig. 4). The dimensionless results $w^*=w/(qL^4/100D)$ and $M^*=M/(qL^2/100)$, where $D=Eh^3/(12(1-\mu^2))$ and L is the plate span, given in the table are related to the displacement and moment results at the center of the clamped plate. Fig. 5 shows that the element QH8-39β converges faster and has higher accuracy. In other numerical tests, we also found that the performance of QH8-39β was better, and here we only list the results of clamped uniformly loaded square plate in Table 7 (Taking into account the layout, data in the table only gives four digits after

Table 8 Central displacements and moments for the clamped square plate subjected to uniform load

h/L	Mesh type	Mesh number				exact
		2×2	4×4	8×8	16×16	
$w_c/(qL^4/100D)$						
	Mesh A	0.149	0.150	0.150	0.150	
0.1	Mesh B	0.154	0.151	0.150	0.150	0.150
	Mesh C	0.158	0.153	0.147	0.149	
	Mesh A	0.126	0.127	0.127	0.127	
0.01	Mesh B	0.131	0.128	0.127	0.127	0.127
	Mesh C	0.135	0.129	0.118	0.124	
	Mesh A	0.126	0.127	0.127	0.127	
$0.001 \sim 10^{-60}$	Mesh B	0.131	0.127	0.127	0.127	0.125
	Mesh C	0.134	0.129	0.117	0.123	
$M_c/(qL^2/100)$						
	Mesh A	2.174	2.280	2.310	2.317	
0.1	Mesh B	2.461	2.347	2.326	2.321	2.31
	Mesh C	2.670	2.395	2.237	2.284	
	Mesh A	2.123	2.249	2.281	2.288	
0.01	Mesh B	2.417	2.317	2.297	2.292	2.291
	Mesh C	2.635	2.364	2.098	2.216	
	Mesh A	2.121	2.248	2.280	2.288	
$0.001 \sim 10^{-60}$	Mesh B	2.416	2.316	2.296	2.292	2.291
	Mesh C	2.635	2.364	2.076	2.193	

the decimal point). Hereinafter, only the element QH8-39β is compared with other reference elements.

7.3.2 Shear locking test

Tables 8 and 9 present the results of the central displacements and moments from thick plate (h/L=0.1) to the very thin plate (h/L=10^{-60}). No matter which mesh is used, it is obvious that the proposed element, QH8-39β is convergent. In addition, the proposed element is free of shear locking. Since the element QH8-21β has the similar character, its numerical results aren't listed here.

7.3.3 Clamped and simply supported square plate under uniform load

The comparison of the presented results with those obtained by other authors is presented in Tables 10 and 11 for the thick and the thin plate, respectively. Convergence of the central displacement and moment for the thick-plate and the thin plate cases are presented in Figs. 6 and 7, with respect to the mesh density (Mesh A in Fig. 4). It can be observed that the present element performs very well in both thick and thin plate situations. Clearly, the new element converges towards the same solution as the elements from the literature, and exhibits an expected faster convergence rate.

Table 9 Central displacements and moments for the simply supported square plate subjected to uniform load

h/L	Mesh type	Mesh number				exact
		2×2	4×4	8×8	16×16	
		$w_c/(qL^4/100D)$				
	Mesh A	0.415	0.424	0.427	0.427	
0.1	Mesh B	0.425	0.427	0.427	0.427	0.427
	Mesh C	0.430	0.428	0.427	0.427	
	Mesh A	0.396	0.404	0.406	0.406	
0.01	Mesh B	0.405	0.406	0.406	0.406	0.406
	Mesh C	0.409	0.407	0.406	0.406	
	Mesh A	0.396	0.404	0.406	0.406	
$0.001\sim10^{-60}$	Mesh B	0.404	0.406	0.406	0.406	0.406
	Mesh C	0.409	0.406	0.406	0.406	
		$M_c/(qL^2/100)$				
	Mesh A	4.527	4.721	4.772	4.784	
0.1	Mesh B	4.865	4.798	4.790	4.789	4.789
	Mesh C	5.104	4.854	4.802	4.792	
	Mesh A	4.518	4.720	4.772	4.784	
0.01	Mesh B	4.857	4.797	4.790	4.789	4.789
	Mesh C	5.101	4.853	4.802	4.792	
	Mesh A	4.518	4.720	4.772	4.784	
$0.001\sim10^{-60}$	Mesh B	4.857	4.797	4.790	4.789	4.789
	Mesh C	5.101	4.853	4.802	4.792	

Table 10 Clamped uniformly loaded square plate: displacement and moment at the center
(a) Thickness-span ration *h/L*=0.1

Element mesh	Zienkiewicz *et al.* (1993)		Auricchio & Taylor (1994)		Miranda & Ubertini (2006)		QH8-39β	
	*w**	*M**	*w**	*M**	*w**	*M**	*w**	*M**
2×2	0.142	2.185	0.142	1.810	0.163	2.838	0.149	2.326
4×4	0.149	2.288	0.148	2.196	0.153	2.448	0.150	2.323
8×8	0.150	2.313	0.150	2.288	0.151	2.351	0.150	2.320
16×16	0.150	2.318	0.150	2.312	0.151	2.323	0.150	2.319
exact	0.150	2.31						

Table 10 (b) Thickness-span ration *h/L*=0.001

Element mesh	Zienkiewicz *et al.* (1993)		Auricchio & Taylor (1994)		Miranda & Ubertini (2006)		QH8-39β	
	*w**	*M**	*w**	*M**	*w**	*M**	*w**	*M**
2×2	0.111	2.179	0.114	1.731	0.137	2.746	0.126	2.121
4×4	0.123	2.260	0.123	2.162	0.129	2.424	0.127	2.248
8×8	0.125	2.282	0.125	2.259	0.127	2.324	0.127	2.280
16×16	0.126	2.288	0.126	2.282	0.126	2.299	0.127	2.288
exact	0.127	2.291						

Table 11 Simple supported (SS2) uniformly loaded square plate: displacement and moment at the center
(a) Thickness-span ration *h/L*=0.1

Element mesh	Ibrahimbegovic (1992)		Soh *et al.* (2001)		Cen *et al.* (2006)		QH8-39*β*	
	*w**	*M**	*w**	*M**	*w**	*M**	*w**	*M**
2×2	0.447	5.591	0.422	5.223	0.413	5.025	0.415	4.527
4×4	0.432	4.979	0.425	4.941	0.420	4.842	0.424	4.721
8×8	0.429	4.836	0.426	4.834	0.425	4.803	0.427	4.772
16×16	0.428	4.8	0.427	4.801	0.426	4.792	0.427	4.784
exact	0.427	4.789						

Table 11 (b) Thickness-span ration *h/L*=0.001

Element mesh	Zienkiewicz *et al.* (1993)		Auricchio & Taylor (1994)		Soh *et al.* (2001)		QH8-39*β*	
	*w**	*M**	*w**	*M**	*w**	*M**	*w**	*M**
2×2	0.403	4.712	0.403	4.119	0.404	5.009	0.396	4.518
4×4	0.405	4.773	0.405	4.623	0.406	4.839	0.404	4.720
8×8	0.406	4.785	0.406	4.747	0.406	4.801	0.406	4.772
16×16	0.406	4.788	0.406	4.778	0.406	4.792	0.406	4.784
exact	0.406	4.789						
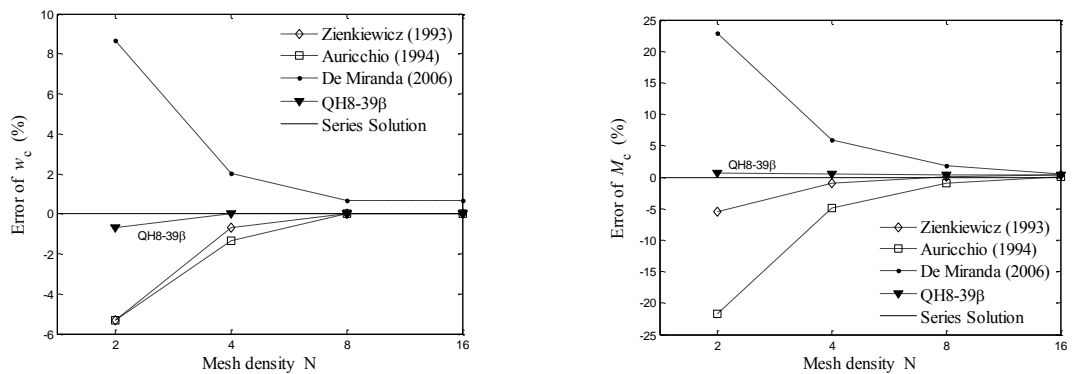
(a) Thick plate (*h/L*=0.1)
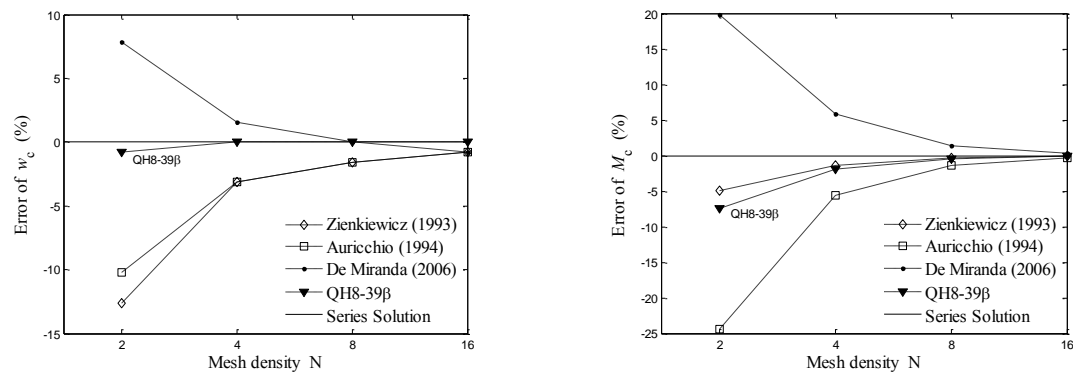
(b) Thin plate (*h/L*=0.001)

Fig. 6 Clamped uniformly loaded square plate (mesh A)-convergence of the center deflection and moment

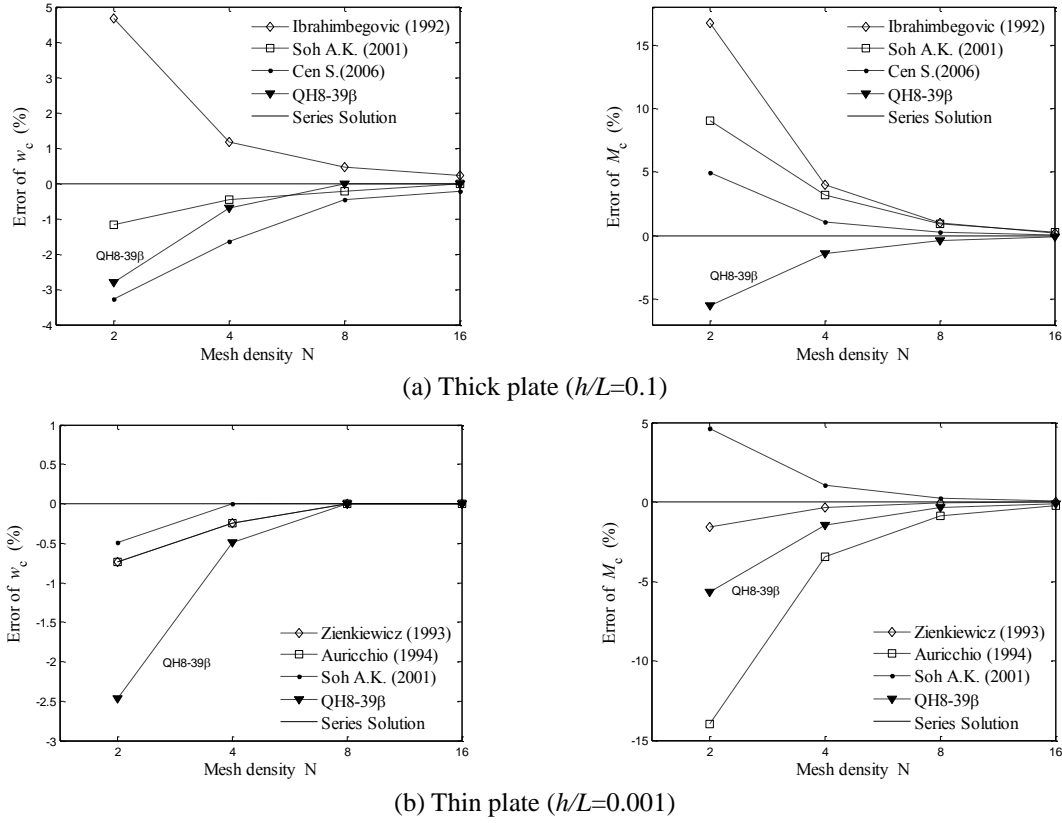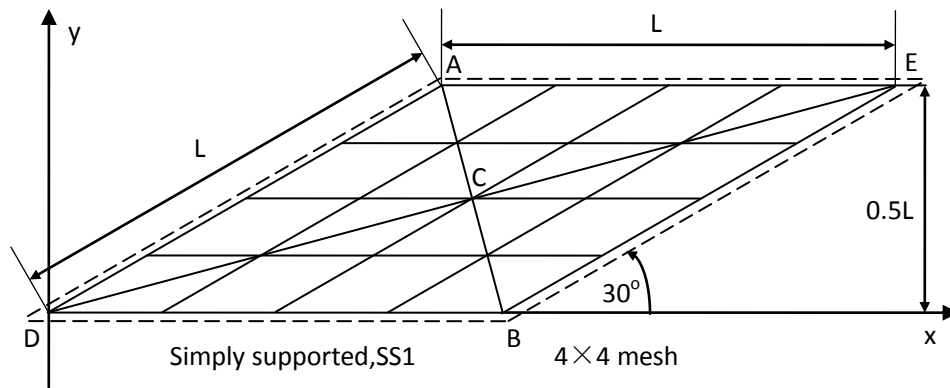(a) Thick plate (*h/L*=0.1)

(b) Thin plate (*h/L*=0.001)

Fig. 7 Simply supported square plate (mesh A)-convergence of the center deflection and moment

Fig. 8 A simply supported (SS1) skew plate under uniform load (mesh density *N*=4)

7.4 Simply supported skew plate

Fig. 8 shows a 4×4 mesh for the simply supported (this time, of the so called soft type SS1) rhombic plate with 30° skew angle and side length *L*=100, subjected to a uniform transversal load *q*=1. The plate possesses the following mechanical properties: *E*=10.92, *μ*=0.3, *k*=5/6. The

dimensionless results $w^*=w/(qL^4/10^4D)$, $M_{11}^*=M_{11}/(qL^2/100)$ and $M_{22}^*=M_{22}/(qL^2/100)$, where $D=Eh^3/(12(1-\mu^2))$, given in the table are related to the displacement and moment results at the center of the plate. This problem is considered as delicate by many researchers. We have studied the problem considering two aspect ratios ($L/h=100$ and $L/h=1000$). The transversal displacement, maximum and minimum bending moments at the center of the plate are given in Tables 12 and 13 for the thick and the thin plate, respectively. Numerical results indicate that the element QH8-39β exhibits excellent performance for skew plate problem as shown in Fig 9. The accuracy and reliability of the proposed element is again clearly illustrated.

7.5 Simply supported circular plate

The circular plate with the simply supported edges SS1 simply supported circular plate of

Table 12 Displacement and principal moments at the center of simply supported skew plate ($L/h=100$)

Element mesh	Soh *et al.* (2001)			Bathe & Dvorkin (1985)			Zienkiewicz *et al.* (1993)			QH8-39β		
	w^*	M_{22}^*	M_{11}^*	w^*	M_{22}^*	M_{11}^*	w^*	M_{22}^*	M_{11}^*	w^*	M_{22}^*	M_{11}^*
4×4	0.754	1.723	2.310	0.359	0.921	1.670	0.513	1.132	2.014	0.418	0.963	1.919
8×8	0.503	1.267	2.067	0.357	0.999	1.782	0.440	1.164	1.992	0.425	1.134	1.941
16×16	0.440	1.169	1.983	0.384	1.046	1.844	0.431	1.155	1.973	0.425	1.143	1.950
32×32	0.423	1.137	1.947	0.404	1.076	1.894	0.427	1.149	1.962	0.424	1.143	1.954
exact	0.423	1.08	1.91									

Table 13 Displacement and principal moments at the center of simply supported skew plate ($L/h=1000$)

| Element mesh	Soh *et al.* (2001)			Bathe & Dvorkin (1985)			Zienkiewicz *et al.* (1993)			QH8-39β		
	w^*	M_{22}^*	M_{11}^*	w^*	M_{22}^*	M_{11}^*	w^*	M_{22}^*	M_{11}^*	w^*	M_{22}^*	M_{11}^*
4×4	0.756	1.73	2.314	0.358	0.921	1.669	0.512	1.133	2.012	0.416	0.966	1.911
8×8	0.506	1.271	2.069	0.343	0.957	1.733	0.439	1.164	1.991	0.422	1.136	1.936
16×16	0.442	1.168	1.985	0.343	0.874	1.717	0.429	1.152	1.967	0.420	1.131	1.938
32×32	0.424	1.136	1.950	0.362	0.923	1.777	0.424	1.140	1.953	0.417	1.122	1.933
exact	0.408	1.08	1.91									
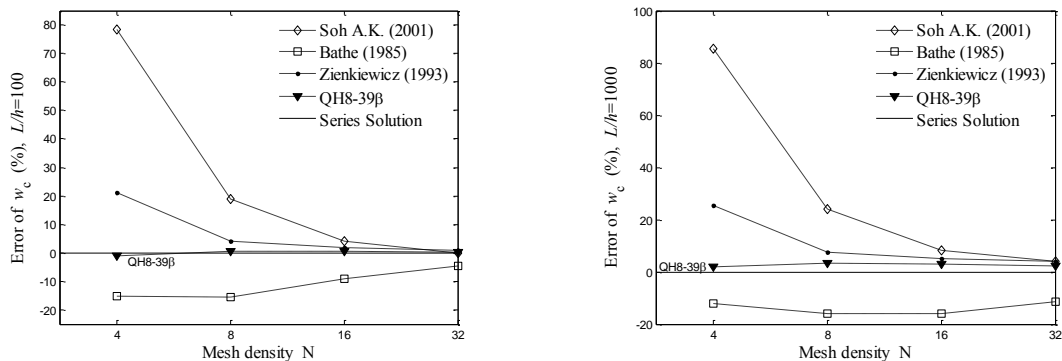
Fig. 9 Convergence test for simply supported (SS1) skew plate
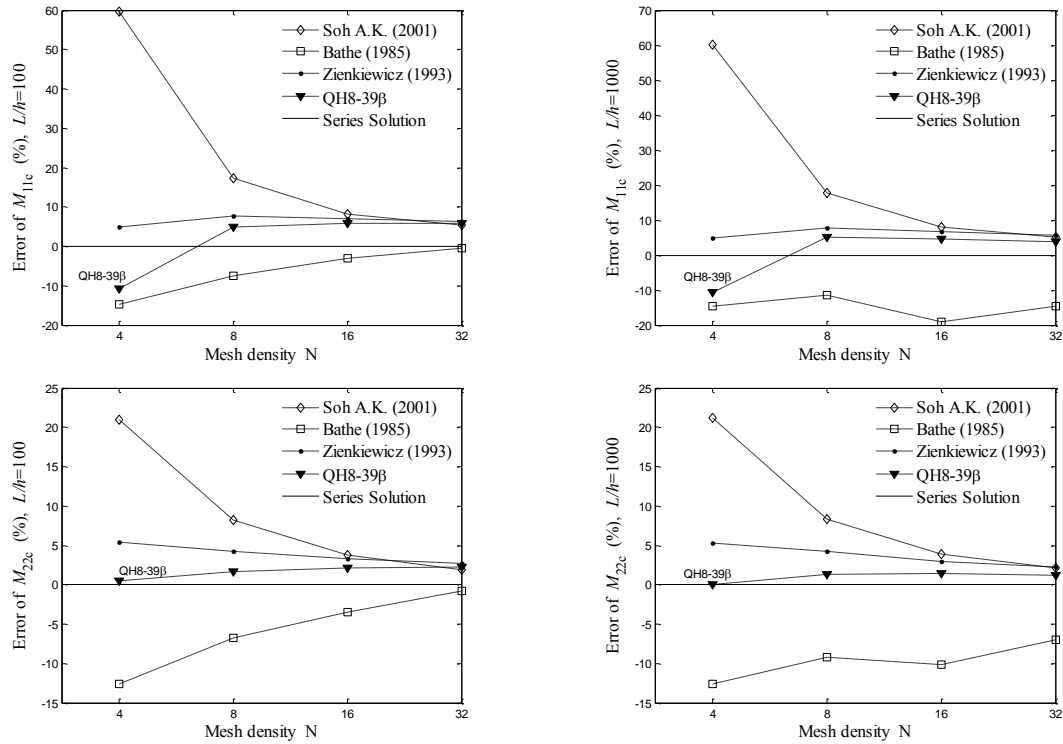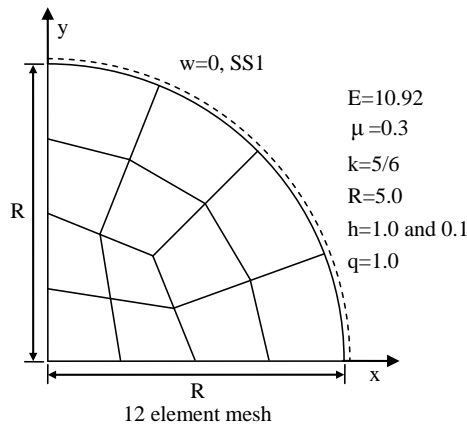
Fig. 9 Continued

Fig. 10 A simply supported (SS1) circular plate under uniform load and mesh

diameter R=0.5 is analyzed next. The plate is subjected to a uniform transversal load q=1 and the following properties are assumed: E=10.92, μ=0.3, k=5/6. Only a quadrant of the plate has been discretized, as reported in Fig. 10, and the results of displacement and bending moment at the plate center in both thick and thin situations are reported in Tables 14 and 15. The present element QH8-39β is compared to some existent elements (Bathe and Dvorkin 1985, Miranda and Ubertini 2006, Katili 1993). It can be observed that the QH8-39β element exhibits excellent performance

Table 14 Simply supported (SS1) circular plate: displacement and moment at the center, *R/h*=5

Element mesh	Bathe & Dvorkin (1985)		Miranda & Ubertini (2006)		Katili (1993)		QH8-39β	
	*w**	*M**	*w**	*M**	*w**	*M**	*w**	*M**
3	0.381	4.78	0.281	5.116	0.396	5.40	0.451	4.638
12	0.407	5.09	0.413	5.168	0.411	5.23	0.429	5.115
48	0.414	5.14	0.415	5.162	0.414	5.18	0.421	5.151
192			0.415	5.158			0.418	5.156
exact	0.416	5.156						

Table 15 Simply supported (SS1) circular plate: displacement and moment at the center, *R/h*=50

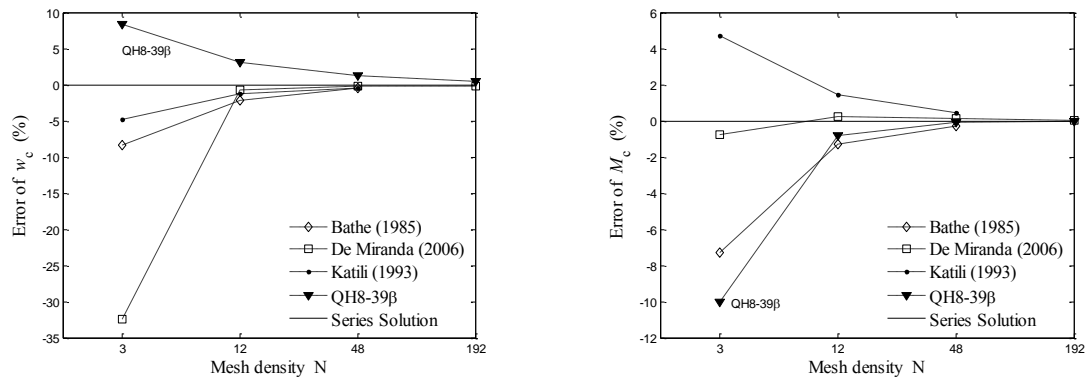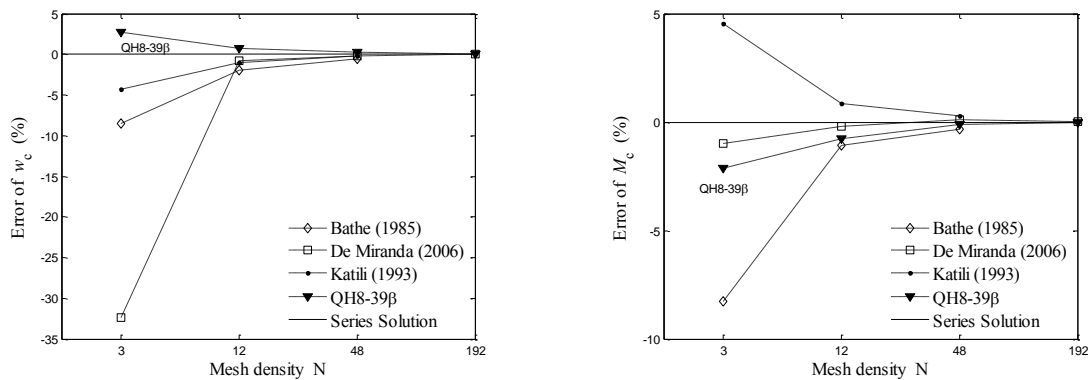| Element mesh	Bathe & Dvorkin (1985)		Miranda & Ubertini (2006)		Katili (1993)		QH8-39β	
	*w**	*M**	*w**	*M**	*w**	*M**	*w**	*M**
3	0.364	4.73	0.269	5.106	0.381	5.39	0.409	5.047
12	0.390	5.10	0.395	5.145	0.394	5.20	0.401	5.116
48	0.396	5.14	0.397	5.161	0.397	5.17	0.399	5.151
192			0.398	5.158			0.398	5.156
exact	0.398	5.156						

(a) Thick plate (*R/h*=5)

(b) Thin plate (*R/h*=50)

Fig. 11 Convergence test for simply supported (SS1) circular plate

for circular plate problem as shown in Fig. 11. Overall good convergence rates are obtained for our new QH8-39β element indeed.

8. Conclusions

In this paper, a new 8-node quadrilateral Mindlin plate element with 24 degrees of freedom is introduced within the framework of hybrid stress element. The proposed element can pass not only the zero shear patch test, but also the non-zero constant shear enhanced patch test. This is the first time to use the hybrid stress method to derive the Mindlin plate element which can pass the non-zero constant shear enhanced patch test.

The arbitrary order Timoshenko beam function is used successfully to derive the boundary displacement interpolation. For the assumed stress field, 39β is adopted instead of 21β since numerical results show that the former is better. Therefore, 39β is suggested to be used for this element.

Moreover, a number of numerical investigations have been carried out to assess the performance of the present element in comparison with some plate elements. Numerical results suggested that the element can be used for the analysis of both moderately thick and thin plates, and the convergence for the very thin case can be ensured theoretically. The element is reliable and free of shear locking.

Acknowledgments

References

Auricchio, F. and Taylor, R.L. (1994), "A shear deformation plate element with an exact thin limit", *Comp. Meth. Appl. Mech. Eng.*, **3**, 393-412.

Ayad, R., Dhatt, G. and Batoz, J.L. (1998), "A new hybrid-mix variational approach for Reissner-Mindlin plate, the MiSP model", *Int. J. Numer. Meth. Eng.*, **42**, 1149-1179.

Bathe, K.J. and Dvorkin, E.N. (1985), "A four node plate bending element based on Mindlin/Reissner plate theory and mixed interpolation", *Int. J. Numer. Meth. Eng.*, **21**, 367-383.

Bathe, K.J. and Dvorkin, E.N. (1986), "A formulation of general shell elements-the use of mixed interpolation of tonsorial components", *Int. J. Numer. Meth. Eng.*, **22**, 697-722.

Bathe, K.J., Iosilevich, A. and Chapelle, D. (2000), "An evaluation of the MITC shell elements", *Comput. Struct.*, **75**, 1-30.

Batoz, J.L. and Lardeur, P. (1989), "A discrete shear triangular nine d.o.f. element for the analysis of thick to very thin plates", *Int. J. Numer. Meth. Eng.*, **29**, 533-560.

Batoz, J.L. and Katili, I. (1992), "On a simple triangular Reissner/Mindlin plate element based on incompatible modes and discrete constraints", *Int. J. Numer. Meth. Eng.*, **35**, 1603-1632.

Bazeley, G.P., Cheung, Y.K., Irons, B.M. and Zienkiewicz, O.C. (1965), "Triangular elements in plate bending conforming and non-conforming solutions", *Proceedings of the Conference on Matrix Methods in Structural Mechanics*, Dayton, Ohio: Wright Patterson Air Force Base.

Belytschko, T. and Tsay, C.S. (1983), "A stabilization procedure for the quadrilateral plate element with one

point quadrature", *Int. J. Numer. Meth. Eng.*, **19**, 405-419.

Cen, S., Long, Y.Q., Yao, Z.H. and Chiew, S.P. (2006), "Application of the quadrilateral area coordinate method: A new element for Mindlin-Reissner plate", *Int. J. Numer. Meth. Eng.*, **66**, 1-45.

Cen, S., Shang, Y., Li, C.F. and Li, H.G. (2014), "Hybrid displacement function element method: a simple hybrid-Trefftz stress element method for analysis of Mindlin-Reissner plate", *Int. J. Numer. Meth. Eng.*, **98**(3), 203-234.

Chen, W.J. (2006), "Enhanced patch test of finite element methods", *Sci. China: Ser. G. Phys-Mech. Astron.*, **49**, 213-227.

Chen, W.J. and Cheung, Y.K. (1987), "A New Approach For The Hybrid Element Method", *Int. J. Numer. Meth. Eng.*, **24**(9), 1697-1709.

Chen, W.J. and Cheung, Y.K. (1996), "The Non-conforming Element Method and Refined Hybrid Method for Axisymmetric Solid", *Int. J. Numer. Meth. Eng.*, **39**(15), 2509-2529.

Chen, W.J. and Cheung, Y.K. (1997), "Refined nonconforming quadrilateral thin plate bending element", *Int. J. Numer. Meth. Eng.*, **40**(21), 3919-3935.

Chen, W.J. and Cheung, Y.K. (2000), "Refined quadrilateral element based on Mindlin/Reissner plate theory", *Int. J. Numer. Meth. Eng.*, **47**, 605-627.

Chen, W.J. and Cheung, Y.K. (2001), "Refined 9-dof triangular Mindlin plate elements", *Int. J. Numer. Meth. Eng.*, **51**, 1259-1281.

Chen, W.J., Wang, J.Z. and Zhao, J. (2009), "The functions for patch test in finite element analysis of Mindlin plate and thin cylindrical shell", *Sci. China: Ser. G. Phys-Mech. Astron.*, **5**, 762-767.

Chen, W.J. and Zheng, S.J. (1998), "Refined hybrid degenerated shell element for geometrically non-linear analysis", *Int. J. Numer. Meth. Eng.*, **41**, 1195-1213.

De Miranda, S. and Ubertini, F. (2006), "A simple hybrid stress element for shear deformable plates", *Int. J. Numer. Meth. Eng.*, **65**, 808-833.

Hughes, T.J.R., Cohen, M. and Haroun, M. (1978), "Reduced and selective integration techniques in finite element analysis of plates", *Nucl. Eng. Des.*, **46**, 203-222.

Ibrahimbegovic, A. (1992), "Plate quadrilateral finite elements with incompatible modes", *Commun. Appl. Numer. Meth.*, **8**, 497-504.

Jelenic, G. and Papa, E. (2011), "Exact solution of 3D Timoshenko beam problem using linked interpolation of arbitrary order", *Arch. Appl. Mech.*, **18**, 171-183.

Katili, I. (1993), "A new discrete Kirchhoff-Mindlin element based on Mindlin-Reissner plate theory and assumed shear strain fields-Part I: an extended DKT element for thick-plate bending analysis", *Int. J. Numer. Meth. Eng.*, **36**, 1859-1883.

Katili, I. (1993), "A new discrete Kirchhoff-Mindlin element based on Mindlin-Reissner plate theory and assumed shear strain fields-Part II: an extended DKQ element for thick-plate bending analysis", *Int. J. Numer. Meth. Eng.*, **36**, 1885-1908.

Lee, S.W. and Pian, T.H.H. (1978), "Improvement of plate and shell finite element by mixed formulation", *AIAA J.*, **16**, 29-34.

MacNeal, R.H. (1978), "A simple quadrilateral shell element", *Comput. Struct.*, **8**, 175-183.

Malkus, D.S. and Hughes, T.J.R. (1978), "Mixed finite element methods-reduced and selective integration techniques: a unification of concepts", *Comp. Meth. Appl. Mech. Eng.*, **15**, 63-81.

Taylor, R.L., Simo, T.C., Zienkiewicz, O.C. and Chan, A.C.H. (1986), "The patch test: a condition for assessing FEM convergence", *Int. J. Numer. Meth. Eng.*, **22**(1), 39-62.

Strang, G. (1972), "Variational crimes in the finite element method", Ed. Aziz, A.R., *The Mathematical Foundations of the Finite Element Method with Applications to Partial Differential Equations*, Academic Press, New York.

Stummel, F. (1979), "The generalized patch test", *SIAM J. Numer. Anal.*, **16**(3), 449-471.

Stummel, F. (1980), "The limitation of the atch test", *Int. J. Numer. Meth. Eng.*, **15**(2), 177-188.

Soh, A.K., Long, Z.F. and Cen, S. (1999), "A new nine DOF triangular element for analysis of thick and thin plates", *Comput. Mech.*, **24**, 408-417.

Soh, A.K., Cen, S., Long, Y.Q. and Long, Z.F. (2001), "A new twelve DOF quadrilateral element for analysis

of thick and thin plates", *Eur. J. Mech. A/Solid.*, **20**, 299-326.

Sze, K.Y. and Chow, C.L. (1991), "A mixed formulation of 4-node Mindlin/Reissner shell/plate element with interpolated transverse shear strains", *Comput. Struct.*, **40**, 775-784.

Soh, A.K., Long, Z.F. and Cen, S. (1999), "A Mindlin plate triangular element with improved interpolation based on Timoshenko's beam theory", *Commun. Numer. Meth. Eng.*, **15**, 527-532.

Wang, M. (2001), "On the necessity and sufficiency of the patch test for convergence of nonconforming finite elements", *SIAM J. Numer. Anal.*, **39**, 363-384.

Zhang, H.X. and Kuang, J.S. (2007), "Eight-node Reissner-Mindlin plate element based on boundary interpolation using Timoshenko beam function", *Int. J. Numer. Meth. Eng.*, **69**, 1345-1373.

Zienkiewicz, O.C. and Taylor, R.L. (1997), "The finite element patch test revisited a computer test for convergence, vali-dation and estimates", *Comput. Meth. Appl. Math. Eng.*, **149**(1-4), 223-254.

Zienkiewicz, O.C., Taylor R.L., and Too, J.M. (1971), "Reduced integration technique in general analysis of plates and shells", *Int. J. Numer. Meth. Eng*., **3**, 275-290.

Zienkiewicz, O.C., Xu, Z., Zeng, L.F., Samuelsson, A. and Wiberg, N.E. (1993), "Linked interpolation for Reissner-Mindlin plate element: Part I-a simple quadrilateral", *Int. J. Numer. Meth. Eng*., **36**, 30433056.

CC